

A Flow Visualization Study on the Movements of Solid Particles Propelled by a Collapsing Cavitation Bubble.

W. K. Soh and B. Willis

Faculty of Engineering
University of Wollongong, New South Wales, 2522 AUSTRALIA

Abstract

The aim of this work is an examination of bubble-particle interaction near a solid boundary in an effort to determine why the addition of particulate to a cavitating flow produces damage that far exceeds that expected by the summation of the cavitation and particulate effects acting independently.

High-speed flow visualization technique is applied to the study of the movements of solid particles induced by the collapse of a cavitation bubble. The captured images of the particles and the cavitation bubble are analysed to provide trajectories and velocity vectors of the particles. The phenomenon points to a possible explanation on the mechanism of cavitation-particulate erosion on solid surfaces.

Introduction

Many of the problems associated with fluid-machinery can be attributed to cavitation erosion. A collapsing vapour bubble produces intense pressure and thermal shock waves, often in combination with violent micro-jets which in 1966 led Benjamin and Ellis [1] to attribute all cavitation damage to these parameters.

Mørch [2,3] reported the collapse of a bubble cloud onto the surface of an ultrasonic vibrator. He noted that bubble collapse was initiated at an outer region of the cloud and propagated inwards, toward the vibrator's surface. Consecutive cavity layers were found to follow in their collapse and generated a converging, spherical pressure wave that acted like an amplifier, for those bubbles collapsing in contact with the vibrator surface. Mørch thus concluded that to some extent the pressure waves are the causes of erosion damage on vibrating surfaces.

The mechanism of cavitation erosion may be explained in terms of the pulsation of a vapour bubble. If a vapour bubble is generated near a surface, it will over-expand and collapse as it moves towards or away from the surface depending on the degree of flexibility of that surface [4], the non-dimensional buoyancy of the bubble and the stand-off distance of the bubble [5]. As the bubble collapses, a liquid jet is formed and threads through the cavity. This liquid jet may impinge on and damage the nearby surface. The magnitude and direction of the momentum carried by the jet is dependent on the dynamic properties of the cavity, its location relative to the surface, the degree of flexibility of the surface and the shape of the surface. Due to the explosive nature of the formation and collapse of the bubble, shock waves travel in liquid outside the cavity and in the vapour inside the cavity. These shock waves may also contribute to the damage of nearby surfaces. The pressure pulses carried by the shock waves will also initiate a sudden collapse of nearby bubbles.

The possibility of particulate 'impurities' contributing to the stimulation of a cavitation bubble's formation, entertained by Weyl and Marboe in 1948 [6], formed the only significant

contribution to research concerning particles and cavitation until recently. Forty-two years later, Wood and Hutton [7] compiled a collection of various papers investigating the nature of the erosion and corrosion caused by cavitation. They concluded that an amplification in a surface's wear rate occurred after the surface was, to some extent, eroded before it was subjected to corrosion.

In 1993, Madadnia and Owen [8] investigated the erosive effects of sand in a sand-laden water flow through fluidic valves. Following the principle of a vortex amplifier, such valves contain no moving parts and consist of a circular chamber with a radial supply port, tangential control port and axial exhaust. Flow control is achieved through combining a small, tangential stream with the radial flow from the supply. By producing a radial pressure gradient, the resistance to flow was dramatically increased and a spiral vortex of fluid was sent down the exhaust port and out of the valve at a somewhat restricted rate.

Flexible castings of the internal passages on both valves were made after one had been exposed to particulate erosion only and the other subjected to a combination of cavitation and particulate erosion. It was evident that the damage caused by erosion was most severe when the flow's cavitation was collapsing, thus it was stated that cavitation significantly affected the abrasive action of the sand (Madadnia and Owen, [8]). Inexplicably, the encountered wear rates were far greater than expected from the summation of individual cavitation and particulate erosion mechanisms.

In 1995, Madadnia and Owen [9] demonstrated that in the flow of liquid through a diffuser, the erosion occurred at the region just down stream of the throat. The erosion rate due to combined particles and cavitation is considerably higher than the erosion solely due to cavitation.

It is envisaged that the collapse of a cavitation bubble may have accelerated particles around the bubble; and the increase of particles' velocities will lead to higher wear rate on surface. It is on this speculation that experiments were carried out to visualize the interaction between particles and a collapsing vapour bubble near a solid wall.

Equipment

The equipment used here is similar to that used by Benjamin and Ellis [1] and by Blake and Gibson [10]. Experiments were carried out in a cavitation tank filled with distilled water and subjected to a spark discharge from a series of capacitors. The discharge of the capacitors was regulated by a silicon controlled rectifier (SCR) or 'Thyratron' that is initiated by the controller of a high-speed camera. Each discharge of the capacitors produces one bubble. The bubble's life cycle was captured by high-speed movie films for detailed analysis.

The cavitation tank has a height of 400 mm and an internal footprint of 277 mm by 300 mm. It is made of acrylic plates of 25 mm in thickness. The lid is sealed with soft rubber gasket (3mm in thickness) coated in vacuum grease and is clamped to

the tank. The tank, designed in this way, will withstand the outside atmospheric pressure when it is evacuated to a pressure of 100 kPa vacuum. By reducing the pressure in the tank, the volume of the generated bubble will be larger in size and has a longer period of pulsation.

The particles used in the experiments were spherical polyethylene bead with an average density of 1374 kg/m³ and a mean diameter of 4mm. The release of a single particle also posed substantial problems in obtaining reliable release that will synchronize with the generation of the bubble. Although the precise timing of a falling particle relative to the age of the bubble could not be determined in advance, a reasonable range of particle-bubble configurations were obtained from many trials.

The NAC E-10 movie camera was used to capture the images of particles and a pulsating bubble. As soon as the filming speed reaches the required framing speed, the controller in the camera initiates the spark discharge and a bubble was generated.

A framing rate of 6000 fps was initially considered to provide the best results when concern was based on the motion of the bubble and the formation of the micro-jet. It was realized that very little movements of the particles were observed and the framing rate was reduced to 4000 fps.

In addition to particles that were released into the water, a number of particles were suspended by light cotton threads and placed close to the tips of the electrodes where the bubble was generated. The aim was to provide additional data on the lateral movements from these suspended beads.

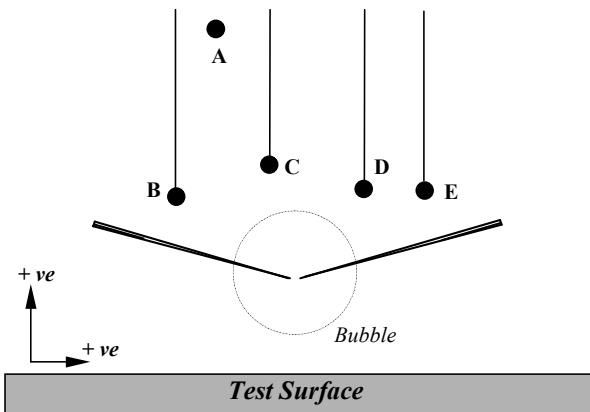


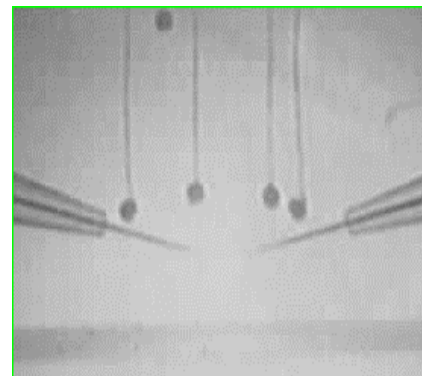
Figure 1 The arrangement of the particles relative to the electrodes for Test 1

The Experiments

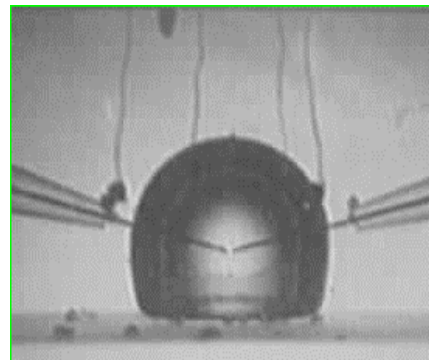
The tips of the electrodes were adjusted to a distance of 13 mm from the floor of the tank. The tank was then sealed and evacuated to an absolute pressure of 20 to 30 Pa. The area of interest was lit by a 2 kW tungsten studio light from the side away from the camera to capture the silhouette in the films.

The exposed films were developed into negatives. Each frame was transferred into a digital image by a digital camera. In the analyses of the images, the known lengths of the protruded tungsten electrodes were used to scale the measurements to the actual length. The mid point between the tips of the electrodes was used as the reference point for all measurements. Although the images were presented in 1024 by 800 pixels, the accuracy of the measurements was restricted by the quality of the image outlines in the films; and the maximum error was found to be 0.2 mm. Larger errors were incurred on the measurement of the centroid since light shading on each particle image varied with time and this affect the apparent shape and size of the particle. It

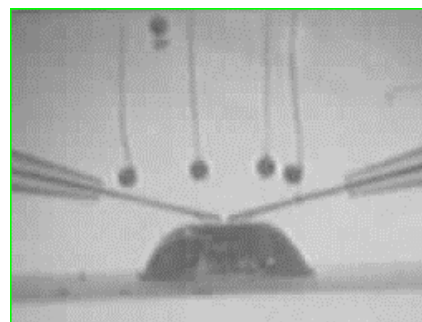
was estimated that the errors in the measurements of the centroids are about 1 mm.



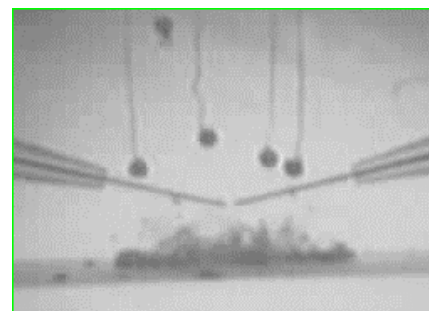
Frame 1 (t = 0.167 ms)



Frame 30 (t = 4.99 ms)



Frame 65 (t = 10.8 ms)



Frame 98 (t = 16.33 ms)

Figure 2 A selection of image frames from Test 1. Note that the particles are virtually stationary during the collapse of the bubble.

The sides of the films were time-marked at 1 kHz. This provides the time parameter of the measured data. At a framing rate of 4000 frames per second, the maximum error in time recording is 0.13 ms.

In Test 1 the arrangement of the particles relative to the bubble is shown in Figure 1. Particle A was released just before the spark

discharge that creates a bubble. In addition to the free falling Particle A, particles B, C, D and E were suspended above the electrodes. Figure 2 shows the movements of these particles as the bubble was generated and collapsed. Within 4 ms the top surface of the bubble grew by a height of 8 mm and in a further 8 ms, the whole bubble collapsed to the floor 13 mm below the reference point. During this time, Particle A fell by a distance of only 6 mm as shown in Figure 2. The average velocity of 0.5 m/s for Particle A is small compared with the average velocity at the top of the bubble, which is 2.88 m/s. Very little movement was observable from particles B, C, D and E.

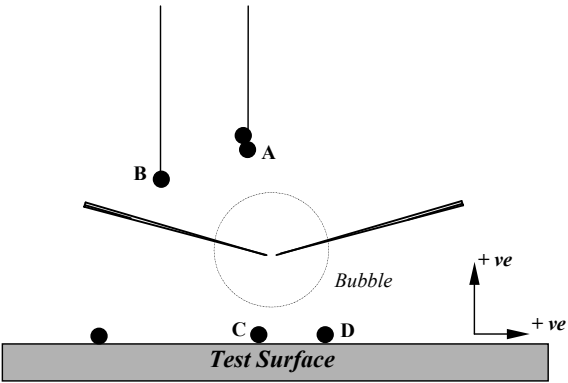


Figure 3 The arrangement of the particles relative to the electrodes for Test 2.

In another example (Test 2), the arrangement of the particle relative to the bubble is shown in Figure 3. In this case, particles C and D were on the tank floor whereas particles A and B were suspended. Figure 5 shows the collapse of the bubble. As the bubble collapsed onto the floor, particles C and D accelerated upward. It is evident that in spite of being in the direct path of the downward action of the collapsing bubble these particles moved upward against the flow of water.

Although the pulsation of a bubble created a high acceleration on the fluid, it had very little influence on the particles that were suspended upward in water. Significant upward movements were observed from particles which were initially on the tank floor. Table 1 contains the essential data for the movements of these particles. A sample for the movement of particle P6 relative to the top surface of the bubble is shown in Figure 4.

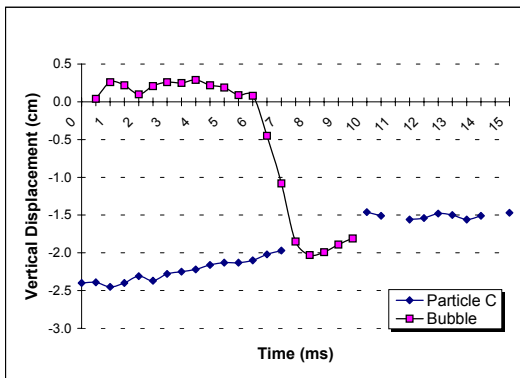
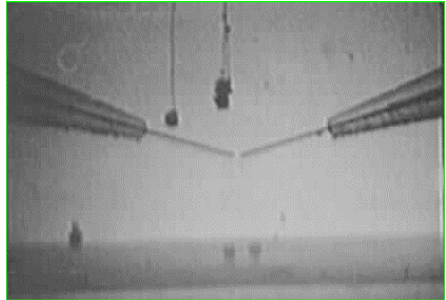
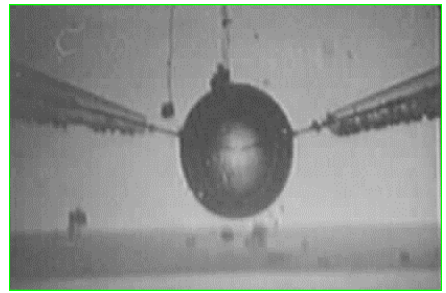


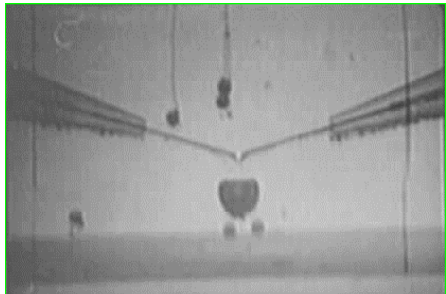
Figure 4 The vertical displacement of Particle C relative to the movement of the top surface of the bubble in Test 2



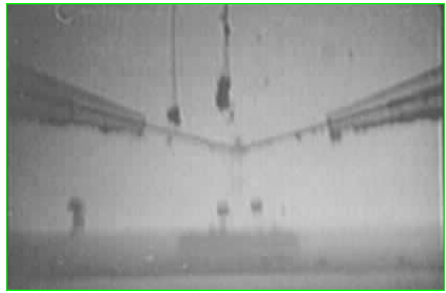
Frame 1 (t = 0.25 ms)



Frame 20 (t = 5 ms)



Frame 28 (t = 7 ms)



Frame 50 (t = 12.5 ms)

Figure 5 A selection of image frames from Test 2. Note the vertical movements of particles C and D (see Figure 2 for the identifications of the particles).

Discussion

The experiments showed very little movements from the suspended particles when the bubble expanded and collapsed. The inability by a pulsating bubble to set a suspended particle in motion implies the absence of pressure drag on the particles. A sudden increase in flow velocities around a particle requires time for the wake to develop. It was only when the wake had grown to a sufficient size that the imbalance of pressure distribution on the particle can produce a significant pressure drag on the particle. The skin friction drag on the particle is expected to be negligible.

In the same way the effect that the flow generated by the bubble has on the particles on the floor is insignificant. Note that the streamlines near the floor were almost horizontal and this is in contrast to the vertical loci of the particles. The initial velocity of the particles, V_0 , may be calculated from their vertical displacement, Y_f , and the time interval of their travels, t_f (given in Table 1) with a further requirement that the average transient drag coefficient, C_D , of these particles be given. The equation is given by:

$$V_0 = \frac{\beta}{\alpha} \left[e^{\alpha Y_f} - \cos(\alpha \beta t_f) \right] \operatorname{cosec}(\alpha \beta t_f)$$

where $\alpha = \sqrt{\frac{3C_D}{4D(s+1)}}$ and $\beta = \sqrt{g \left(\frac{s-1}{s+1} \right)}$

and s and D are the specific gravity and diameter of the particles (1.734 and 4 mm respectively).

The transient drag coefficient may be estimated from the steady state data. From the range of the Reynolds numbers of the particles ranging from 500 to 8000 (Table 1), the steady state drag coefficient is in the range of 0.5 to 1.0. The initial velocities of the particles are shown in Table 1.

The question on how the particles on the floor acquired their initial velocity has to be answered. If the flow of the fluid plays no part in accelerating the particles, then it is possible that the vibration of the floor resulting from the impact caused by collapse of the bubble. Let A be the amplitude of the vibration and the acceleration a_y that will produce the required initial velocity V_0 of a particle is given by:

$$a_y = V_0^2 / A$$

Since the amplitudes of the floor vibration were not visible in the films, it must be less than the error of the special measurement, 0.2 mm. By overestimating the amplitude the calculation will yield a lower than expected values for the acceleration. For example, using $C_D = 0.5$ in a floor amplitude of 1.0 mm, the values for the accelerations were estimated to vary from 15 m/s² (for $V_0 = 0.12$ m/s) to 3087 m/s² (for $V_0 = 2.15$ m/s).

The accurate value for the acceleration of the floor can only be calculated from the analysis of elastic vibration of the floor material resulting from the high-pressure impact of the bubble. However, the flow visualization study has shown that the vibration of the floor resulting from the impact of the bubble may contribute to the abrasive wear on surface by the particles that are in contact with the floor. Since the acceleration by the floor increases the contact force between the particle and the floor, the wear rate of the surface will be proportionately increase. This may be the reason for the high erosion rate in a particulate-laden cavitating flow that was reported by Madadnia and Owen in 1993.

Concluding Remarks

This simple visualization study showed that the highly accelerated transient flow created by the collapse of a cavitation bubble was unable to propel the particles that were in suspension and in free fall. Hence it is not likely that particles can be propelled by the flow toward a solid wall to cause wear by collision.

On the other hand, the particles that were in contact with the floor started moving upward as soon as the bubble collapsed onto the floor. The estimated initial accelerations of these particles, subjected to errors of the measurements, were remarkably large. The initial acceleration of the particles was a result of the vibration of the tank floor set up by the collapse of the bubble. This led to a suggestion that the high contact forces between the

floor and the particles may be the reason for the high erosion rate experienced in a particulate-laden cavitation flow.

References

- [1] Benjamin, T.B. & Ellis, A.T., The Collapse of Cavitation Bubbles and the Pressure Thereby Produced Against Solid Boundaries, *Phil. Trans. R. Soc. Lond.* **A260**, 1966, 221-240.
- [2] Mørch, K.A., On the Collapse of Cavity Clusters in Flow Cavitation, *Cavitation and Inhomogenities in Underwater Acoustics*, editor. W. Lauterborn, 1980, 95-100.
- [3] Mørch, K.A., Energy Consideration on the Collapse of Cavity Clusters, *Appl. Sci. Res.*, **38**, 1982, 313-321.
- [4] Gibson D. C., Cavitation Adjacent to Plane Boundaries, *Proc. Third Australian Conf. on Hydraulics and Fluid Mechanics, Institution of Engineers, Australia*, 1968, 210-214.
- [5] Best, J. P. and Blake, J. R., An Estimate of the Kevin Impulse of a Transient Cavity, *J. Fluid Mech.*, **261**, 1994, 75-93.
- [6] Weyl, W.A. and Marboe, E.C., Some Mechano-Chemical Properties of Water, US Office of Naval Report, 1948.
- [7] Wood, R.J.K. and Hutton, S.P., The Synergistic Effects of Erosion and Corrosion: Trends in Published Results, *Wear*, **140**, 1990, 387-394.
- [8] Madadnia, J. and Owen, I., Accelerated Surface Erosion by Cavitating Particulate Laden Flows, *Wear*, **165**, 1993, 113-116.
- [9] Madadnia, J. and Owen, I., Erosion in Conical Diffusers in Particulate-Laden Cavitating Flow, *Int. J. Multiphase Flow*, **21**, 1995, 6, 1253-1257.
- [10] Blake, J.R. and Gibson, D.C., Growth and Collapse of a Vapour Cavity Near a Free Surface, *J. Fluid Mech.*, **111**, 1981, 123-140.

Particles	P1	P2	P3	P4
X	1.7	8	4	1.1
Y_f	1.4	1.2	1.4	1.8
t_f	13.0	10.0	10.0	9.3
V_{av}	0.11	0.12	0.14	0.19
Re_D	592	660	769	1064
V_0	0.121	0.131	0.152	0.208

Particles	P5	P6	P7
X	0.9	23.9	22.8
Y_f	7.9	9.3	9.4
t_f	16.0	8.5	6.5
V_{av}	0.49	1.09	1.45
Re_D	2714	6013	7948
V_0	0.593	1.330	1.757

Table 1 Data for particles initially on the tank floor. P6 and P7 are particles C and D respectively from Test 2

X	Initial horizontal distance from the centreline (mm)
Y_f	Vertical distance travelled (mm)
t_f	Time interval (ms)
V_{av}	Average velocity (m/s)
Re_D	Reynolds number
V_0	Calculated initial velocity (m/s)